IEEE Photonics Journal
An IEEE Photonics Society Publication

Open Access

Polarization Modulation Instability in All-Normal Dispersion Microstructured Optical Fibers With Quasi-Continuous Pump

Volume 11, Number 5, October 2019

Abraham Loredo-Trejo
Yanelis López-Diéguez
Lorena Velázquez-Ibarra
Antonio Díez
Enrique Silvestre
Julian M. Estudillo-Ayala
Miguel V. Andrés

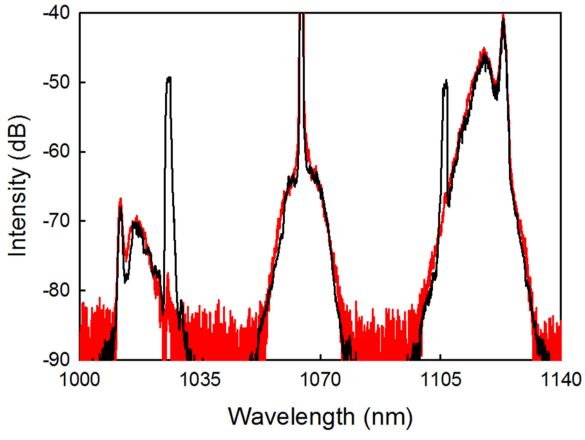

DOI: 10.1109/JPHOT.2019.2944063

IEEE photonics SOCIETY

IEEE

Polarization Modulation Instability in All-Normal Dispersion Microstructured Optical Fibers With Quasi-Continuous Pump

Abraham Loredo-Trejo,[1] Yanelis López-Diéguez,[1,2] Lorena Velázquez-Ibarra,[1,3] Antonio Díez,[1] Enrique Silvestre,[4] Julian M. Estudillo-Ayala,[2] and Miguel V. Andrés[4]

[1]Departamento de Física Aplicada y Electromagnetismo—ICMUV, Universidad de Valencia, Burjassot 46100, Spain
[2]División de Ingenierías Campus Irapuato, Departamento de Electrónica, Universidad de Guanajuato, Salamanca 36885, México
[3]Departamento de Física, Universidad de Guanajuato, León 37150, México
[4]Departamento de Óptica—ICMUV, Universidad de Valencia, Burjassot 46100, Spain

DOI:10.1109/JPHOT.2019.2944063

Manuscript received July 25, 2019; revised September 16, 2019; accepted September 20, 2019. Date of publication October 2, 2019; date of current version October 8, 2019. The work of Y. López-Diéguez was supported in part by Consejo Nacional de Ciencia y Tecnología (577494/307127) and in part by DAIP Universidad de Guanajuato. This work was supported by Ministerio de Economía y Competitividad (MINECO) and in part by the Fonds Européen de Développement Économique et Régional (FEDER) (TEC2016-76664-C2-1-R). Corresponding author: Antonio Díez (email: antonio.diez@uv.es).

Abstract: We report the experimental observation of the polarization modulation instability (PMI) effect in all-normal dispersion (ANDi) microstructured optical fibers (MOFs) with quasi-continuous pumping. The small unintentional birefringence ($\sim 10^{-5}$), that any realistic non-polarization maintaining MOF exhibits, contributes to this nonlinear effect. PMI can produce two sidebands whose polarization state is orthogonal to the polarization of the pump. In this work, only one type of PMI process is observed, i.e., when the pump is polarized along the slow axis of the fiber and sidebands are generated in the fast axis mode. This PMI process was studied experimentally in two ANDi fibers with different dispersion features and pumped with long (700 ps) pump pulses at 1064 nm. Experimental results are compared with theoretical calculations, with reasonably good agreement.

Index Terms: Microstructured optical fibers, Chromatic dispersion, Fiber nonlinear optics, Four-wave mixing, Optical polarization.

1. Introduction

Polarization modulation instability (PMI) is a form of modulation instability that affects the polarization state of light that propagates through the fiber [1]–[4]. PMI can exist in weakly birefringent optical fibers, but also in isotropic fibers with almost zero birefringence [5]. In weakly birefringent fibers, the effect occurs when one of the linearly polarized eigenmodes (fast or slow) of the birefringent fiber is excited with an intense optical pump signal. Some remarkable aspects of this nonlinear effect are: (i) the polarization state of the light generated through PMI is orthogonal to the polarization state of the pump signal, and (ii) it can occur even when the fiber is pumped in the normal dispersion regime. For this nonlinear phenomenon, the contribution of the fiber birefringence to the linear phase mismatch

plays a major role in the phase-matching condition [1]–[4]. PMI features in weakly birefringent fibers pumped in normal dispersion are quite different depending on whether the pump is polarized along the slow or the fast axis of the fiber. In the first case, PMI produces sidebands separated from the pump regardless of the pump power. For fast axis pumping, a low-power threshold exists for PMI generation, the gain profile only shows sidebands detuned from the pump at high pump powers, and the gain at zero detuning does not vanish regardless of the pump power level [1]–[4]. The first experimental observation of PMI in low-birefringence optical fibers pumped in normal dispersion was reported in 1995 [2]. Experiments were conducted with conventional single-mode fibers that were pumped with intense red pulses in the normal dispersion regime. Weak birefringence was introduced in the fibers by fiber bending.

Frequency detuning of PMI sidebands depends on the fiber birefringence as shown in [2], but also on the chromatic dispersion of the fiber. The dependence of frequency detuning on the fiber dispersion is particularly notable for low values of dispersion [2], [4]. Widely spaced PMI sidebands can be generated in low birefringent fibers pumped on the slow axis of the fiber when the fiber dispersion at the pump wavelength is normal and close to zero. This can be of interest in fields such as new light source development with special emission characteristics suited for specific applications [6]. In this sense, microstructured optical fibers (MOFs) can be a platform for generation of widely spaced bands based on PMI, because of the high flexibility for dispersion engineering in MOFs [7].

In the context of MOFs, PMI was first observed in the normal dispersion regime in a large-air-filling fraction MOF with a conventional dispersion profile with one zero-dispersion wavelength (ZDW), which was pumped near the ZDW [8]. PMI sidebands were generated at 568.5 and 751.5 nm when pumped at 647 nm. In this fiber, additional widely spaced bands due to scalar four-wave mixing (FWM) were simultaneously generated [9]. This feature, i.e., the simultaneous generation of FWM and PMI, will occur in fibers with a dispersion profile including ZDWs when they are pumped in normal dispersion near the ZDW since phase-matching for scalar FWM is also often accomplished. This can be avoided by the use of all-normal dispersion (ANDi) fibers, in which the chromatic dispersion remains normal over the entire wavelength region of interest, without any ZDW. In this type of fibers, neither scalar FWM nor scalar MI can be generated [1]–[4] since phase-matching is not accomplished for any pump wavelength.

In the last years, the potential of ANDi MOFs as nonlinear media has been widely investigated. They have been proposed as a platform for the formation of femtosecond parabolic pulses by means of passive nonlinear reshaping [10]. However, most of the interest on ANDi fibers comes from their ability for the generation of coherent, octave-spanning, and recompressible supercontinuum (SC) light [11]–[18]. It has been demonstrated experimentally with pump pulses in the fs temporal regime [11]–[16], and further analysis has shown that octave-spanning SC spectra with high temporal coherence could be achieved with pump pulse durations in the ps regime [18]. In recent works, however, it was found that polarization induced noise can degrade the coherence of ANDi femtosecond supercontinuum [19], [20]. PMI assisted by the weak unintentional birefringence of the fibers has been identified as the origin of such coherence degradation. The use of polarization-maintaining ANDi fibers has been proposed to avoid such limitations [20].

In this paper, we report the experimental investigation of PMI effect in weakly birefringent ANDi MOFs with quasi-CW pumping at 1064 nm. As mentioned before, PMI in ANDi MOFs has been observed previously in the femtosecond pump regime [19], [20]. However, it is expected that the nonlinear dynamics will show differences when pumping with long pump pulses instead of fs pulses. To our knowledge, an experimental study of PMI in ANDi MOFs with long pump pulses has not been carried out so far. In this work, we investigate this effect using pulses with pulse duration much longer than the observed modulation period and, simultaneously, with spatial pulse extension along the fiber of the same order of magnitude than the fiber polarization beatlength.

2. PMI in ANDi MOFs

The effect of PMI in optical fibers can be analyzed by a vector theory of four-wave mixing, where the polarization states of light, as well as the birefringence of the fiber are taken into account. The

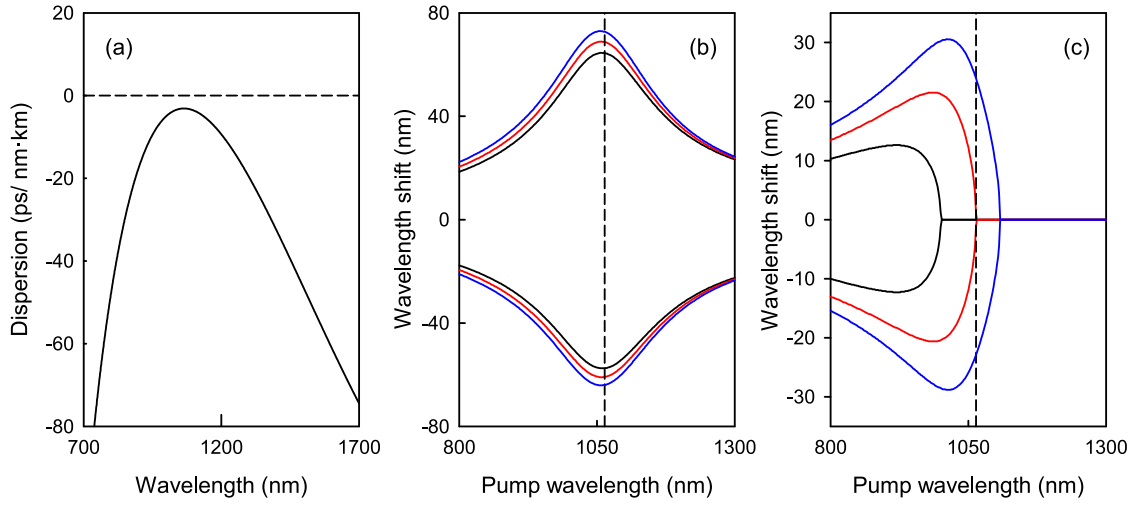

Fig. 1. (a) Chromatic dispersion vs. wavelength for a weakly birefringent MOF. Parametric wavelengths for (b) S-F PMI, and (c) F-S PMI at different pump powers, $P_p = 1.5{\cdot}P_{th}$ (black), $P_p = 2{\cdot}P_{th}$ (red), and $P_p = 2.5{\cdot}P_{th}$ (blue), being $P_{th} = 1.81$ kW. Fiber parameters: $\Lambda = 1.5$ μm, d/$\Lambda = 0.43$, $B_p = 1{\times}10^{-6}$. Vertical dashed line indicates the MDW.

net phase mismatch and the energy conservation relations can be used to calculate the spectral shift of the sidebands [1], [4], [21]. Fig. 1 shows the parametric wavelengths as a function of pump wavelength for the different FWM/MI processes of a weakly birefringent ANDi MOF, for different pump powers. Linearly polarized light with polarization orientation aligned to the principal axes of the fiber, fast (F) and slow (S), was considered in the calculations. Solutions for two different interactions were found in this type of fiber. S-F and F-S correspond to the case in which the generated Stokes and anti-Stokes photons have the same polarization, but orthogonal to the polarization of the pump photons. In particular, for the S-F/F-S interaction, two slow/fast photons of the pump give rise to two fast/slow Stokes and anti-Stokes photons. These two solutions correspond to what is known as PMI processes. As expected, no solutions were found for FWM/MI processes in which the polarization of pump and generated photons is the same, as it corresponds to a fiber with no ZDW.

In the case of S-F process (see Fig. 1(b)), the largest wavelength shift is obtained when the fiber is pumped at the wavelength that matches the maximum of the dispersion curve (MDW), i.e., at the wavelength at which the fiber dispersion is minimum. The lower is the dispersion at the MDW, the wider is the wavelength spacing of the S-F PMI bands for that pump wavelength. The calculated bands shift slightly with pump power, P_p. The results for the F-S PMI process are somehow more complex (see Fig. 1(c)). As it is known, this PMI process exhibits a power threshold $P_{th} = 3 \cdot B_p A_{eff} / 2\, n_2$, where B_p is the phase birefringence, A_{eff} is the effective area, and n_2 is the nonlinear refractive index. When $P_p < P_{th}$, the effect cannot be produced. When $P_{th} < P_p < 2P_{th}$, a band centered at zero detuning is generated. Sidebands start to appear when $P_p > 2\, P_{th}$. More details can be found in [1]–[4].

3. Fiber Characteristics and Experimental Setup

We carried out several experiments to investigate PMI generation in ANDi MOFs with quasi-CW pumping. Two ANDi fibers were used in the experiments. They were fabricated following the stack-and-draw technique. Inset of Fig. 2 shows a scanning electron microscope (SEM) image of the cross section of the fibers. The cladding is formed by a triangular lattice of air holes of the same diameter, and the core is just a missing hole. The structural parameters of the fibers, i.e., air hole diameter d and pitch Λ are given in Table 1. Both fibers are single mode at the wavelength range of the experiments. The chromatic dispersion of the fibers was measured experimentally using the

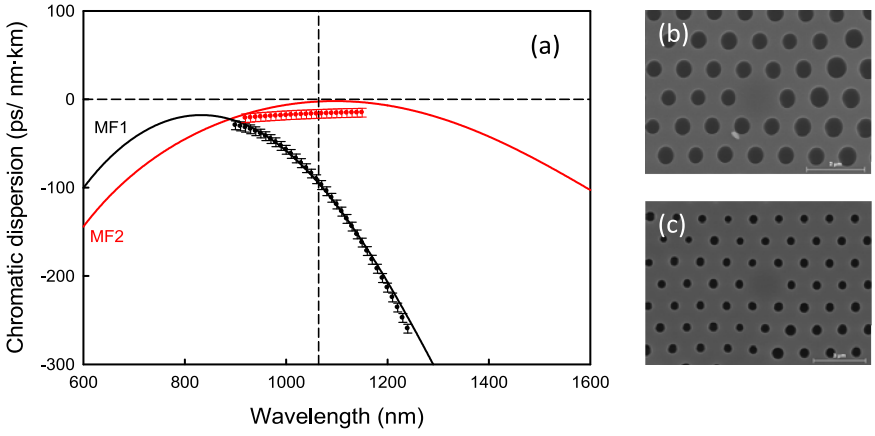

Fig. 2. (a) Chromatic dispersion vs. wavelength of the fibers used in the experiments. Dots are experimental measurements and solid lines are theoretical calculations. SEM images of the fibers' cross-section: (b) MOF1, (c) MOF2.

TABLE 1
Structural Parameters, Chromatic Dispersion, Group Birefringence, and Effective Area of the MOFs at 1064 nm

	Λ (μm)	d/Λ	D (ps/nm km)	B_g ($\times 10^{-5}$)	A_{eff} (μm^2)
MOF1	1.0	0.52	-100	1.2	9.4
MOF2	1.6	0.37	-21	1.1	25

interferometric method described in [22]. Fig. 2 shows the chromatic dispersion as a function of wavelength for the two fibers, along with the simulation results obtained from theoretical modelling carried out using the method reported in [7]. The structural parameter values included in Table 1 were used for the calculations. The dispersion of the two fibers shows the typical convex profile of ANDi fibers with normal dispersion for all wavelengths. The MDW values are 820 nm and 1090 nm, for MOF1 and MOF2, respectively. The experimental values of dispersion at the pump wavelength used in the experiments, i.e., 1064 nm, are summarized in Table 1.

In principle, MOFs with regular triangular lattice of identical, circular air holes are non-birefringent fibers. However, realistic fibers exhibit a small amount of residual birefringence due to imperfections in the resulting microstructure, and the finite number of air holes rings. The group birefringence B_g of both fibers was characterized using the technique described in [23]. Results are summarized in Table 1.

Fig. 3 shows the arrangement used in the experiments. A diode pumped passively Q-switched Nd:YAG microchip laser (TEEM Photonics SNP-20F-100) that emits pulses at 1064 nm of 700 ps duration (FWHM), few kW of peak power, and a repetition rate of 19.1 kHz was used as the pump for the nonlinear experiment. The spectral bandwidth is smaller than 30 pm (FWHM). Inset of Fig. 3 shows the temporal shape of the pump pulses. Assuming a group velocity of 2×10^8 m/s the pulse spatial width is about 14 cm. The pump beam was launched into a short section of the fibers under test (FUT). Typical fiber length used in the experiments was $\sim$50 cm. The laser emission is linearly polarized, with a polarization extinction (PER) of 32 dB. A half-wave plate (HWP) was positioned at the laser output, in order to rotate the polarization plane of the launched pump beam with respect to the fiber axes. A linear polarizer was used in part of the experiments, to analyze the polarization of the output light.

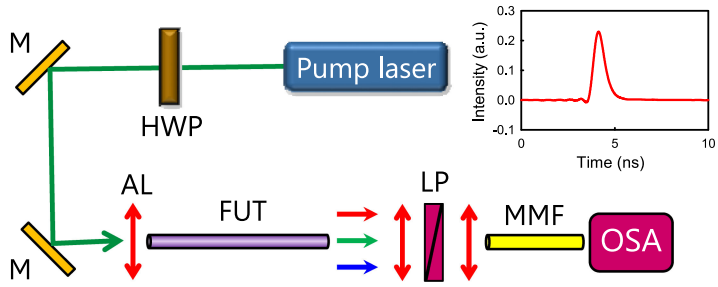

Fig. 3. Experimental arrangement. M: mirror; HWP: half-wave plate; AL: aspheric lens (x30); FUT: fiber under test; LP: linear polarizer; MMF: multimode collecting fiber; OSA: optical spectrum analyzer. Inset shows the temporal shape of the pump pulses.

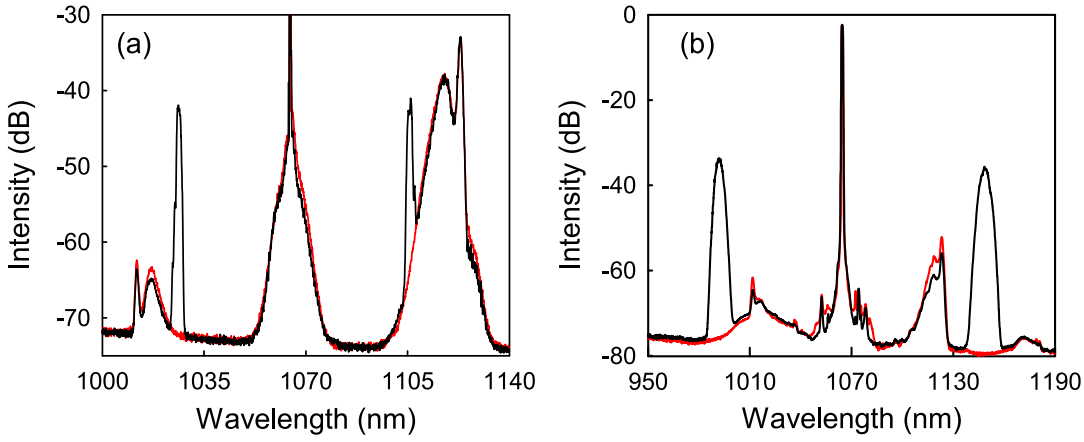

Fig. 4. Spectra for two orthogonal polarizations orientations of the pump: (black) pump polarization orientation adjusted to obtain maximum PMI generation efficiency, and (red) pump polarization rotated 90° with respect to the previous. (a) MOF1, 30 mW pump power. (b) MOF2, 23 mW pump power.

4. Experimental Results and Discussion

The spectrum of the light exiting the fibers was analyzed for different pump powers and polarization orientations of the pump. Fig. 4(a) shows an example for two orthogonal orientations of the pump polarization, and identical pump power obtained from MOF1. Along with the pump laser centered at 1064 nm, one can observe several nonlinear features. For both HWP angles, Stokes and anti-Stokes Raman scattering was generated. Additionally, two bands centered at 1026 nm and 1105 nm, are shown for one of the polarization orientations. Similarly, in the case of MOF2 a pair of narrow bands centered at 966 nm and 1184 nm was observed (see Fig. 4(b)). Such bands result from the S-F PMI process, as we confirmed experimentally, and backed by theoretical modelling (see discussion below).

We studied the polarization of the PMI sidebands by analyzing the polarization of the light exiting the fiber using a broadband bulk linear polarizer. Prior the insertion of the linear polarizer, the orientation of the HWP was adjusted to achieve the highest amplitude of the PMI bands. Then, the pump power launched into the fiber and the orientation of the HWP were kept constant during the rest of the experiment. The linear polarizer was inserted at the fiber exit. The light transmitted through the polarizer was collected by a multimode fiber and analyzed with the optical spectrum analyzer. Light spectra were recorded for different orientations of the polarizer axis. The amplitude of the different spectral components varied in different ways with the orientation of the polarizer. Fig. 5 shows the spectrum obtained when the polarizer was oriented so that the amplitude of the PMI bands was optimized. Starting from this orientation, rotation of the polarizer produced the

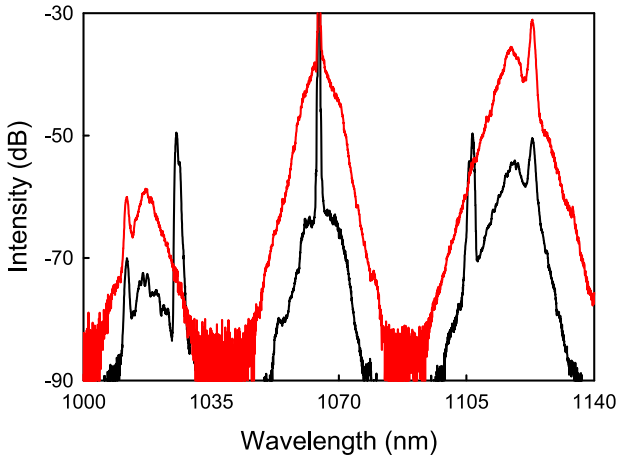

Fig. 5. Spectra of light leaving the fiber after passing through a linear polarizer, for two different orientations of the polarizer: (black) orientation of the polarizer adjusted to obtain the best PMI amplitude, and (red) polarizer orientation rotated 90° with respect to the previous. Fiber: MOF1.

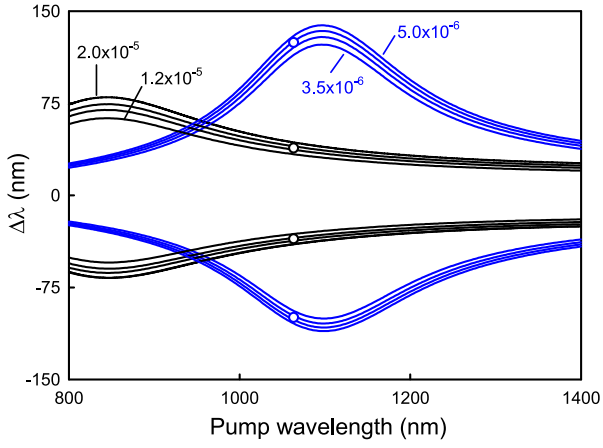

Fig. 6. Wavelength shift of S-F PMI Stokes and anti-Stokes bands vs. pump wavelength, for different values of B_p. Solid lines are theoretical calculations, and dots are experimental data. MOF1 (black) and MOF2 (blue). Phase birefringence values used in theoretical calculations are indicated.

reduction of the amplitude of the PMI bands and, simultaneously, the increase of the amplitude of the rest of spectral components. The red line corresponds to a 90° rotation of the polarizer from the initial position. The PMI bands are completely filtered, while the rest of spectral components, including the pump laser line and Raman bands, increased in amplitude few tens of dB (which agrees with the PER of the polarizer). This result confirms that the polarization of the PMI bands is orthogonal to the polarization of the pump laser, as it corresponds to the PMI process.

Fig. 6 shows the theoretical calculations of the wavelength shift from the pump wavelength of S-F PMI bands, as a function of pump wavelength, for the specific fibers of the experiments. Different phase birefringence values B_p were considered for the calculations of the phase-matching wavelengths. A value of nonlinear refractive index for silica $n_2 = 2.7\times10^{-20}$ m^2/W was used for the calculations. The experimental Stokes and anti-Stokes wavelengths, obtained at 1064 nm are also included for both fibers. Best agreement between theoretical calculations and experimental data is achieved for $B_p = 1.8 \times 10^{-5}$ and $B_p = 4.5 \times 10^{-6}$, for MOF1 and MOF2, respectively. Notice that the birefringence values obtained from the fitting differ from the birefringence values included in

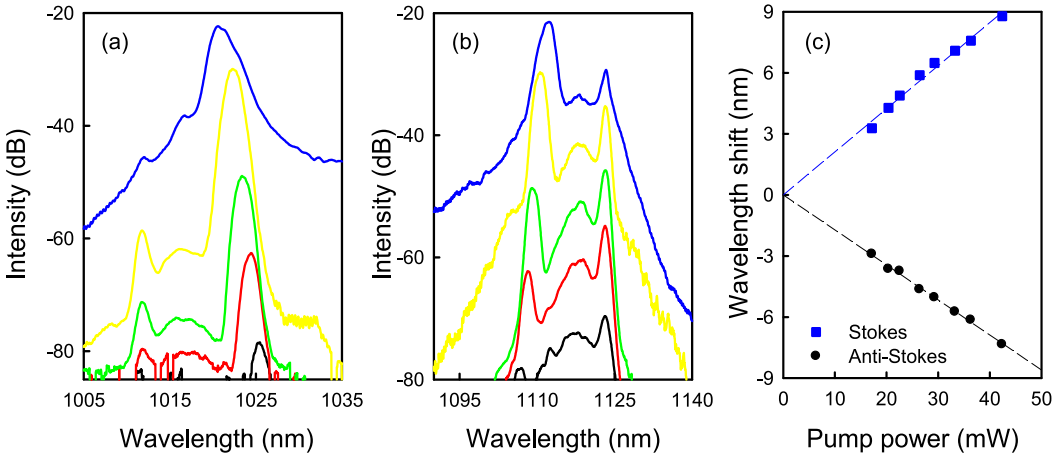

Fig. 7. (a)-(b) Spectrum of light at the wavelength range around the anti-Stokes and Stokes bands, respectively, for increasing pump power. (c) Wavelength shift as a function of pump power. Dots are experimental data. Dashed lines are a guide to the eye.

Table 1, which correspond to group birefringence. Although both parameters give information about the birefringent properties of the fibers, they are not exactly the same magnitude. The corresponding beatlentghs are 5.9 cm and 23.6 cm, respectively, which are of the same order of magnitude than the pulse extension on the fiber.

Fig. 7(a)–(b) shows the spectrum around the PMI bands generated in MOF1, as a function of the input pump power. The HWP was adjusted to optimize PMI bands. As expected, all the frequencies generated by the different nonlinear mechanisms increase in amplitude. Additionally, we can notice that, unlike Raman features, the PMI bands shift slightly. They move away from the pump wavelength as the pump power increases, few nanometers for the pump wavelength range of the experiments. Fig. 7(c) summarizes the shift of the Stokes and anti-Stokes PMI wavelengths as a function of pump power. The PMI bands shift with pump power as a result of the contribution of the nonlinear term to the phase mismatch [1]–[4].

As shown in Fig. 4, PMI was not observed in any of the fibers when they were pumped in the fast axis. This agrees with what it is expected since estimated values of P_{th} are 9.4 kW and 6.4 kW for MOF1 and MOF2, respectively, and in our experimental arrangement the largest value of peak power that could be launched into the fiber was around 4 kW, which is far below such P_{th} values.

5. Conclusions

In summary, we have reported the experimental observation of PMI generation in ANDi MOFs with quasi-continuous pump. In ANDi fibers, phase-matching for scalar FWM/MI is not accomplished. In principle, two PMI process are possible. However, F-S PMI presents a power threshold that was not reached in our experiments. Small birefringence of the order of 10^{-5}, which in realistic fibers can be provided simply by residual birefringence, contributes significantly to the phase-matching condition. We have shown that widely spaced sidebands can be obtained by this nonlinear mechanism with proper fiber designs. This nonlinear effect was investigated in two ANDi MOFs with different dispersion profiles using long pump pulses (700 ps) at 1064 nm. Anti-Stokes and Stokes PMI bands centered at 1026 nm and 1105 nm for MOF1, and 966 nm and 1184 nm for MOF2, were observed when the fibers were pumped in the slow axis mode. The experimental PMI wavelengths are in reasonable good agreement with theoretical calculations. Sidebands generated through PMI can eventually be exploited for the development of new light sources based on this effect. Furthermore, PMI can seriously deteriorate the coherence characteristics of supercontinuum spectra generated using ANDi fibers with quasi-CW pump, although pump polarization control can reduce the drawbacks of PMI by matching the fast axis with power levels below F-S PMI threshold.

References

[1] S. Wabnitz, "Modulational polarization instability of light in a nonlinear birefringent dispersive medium," *Phys. Rev. A.*, vol. 38, pp. 2018–2021, 1988.

[2] S. G. Murdoch, R. Leonhardt, and J. D. Harvey, Polarization modulation instability in weakly birefringent fibers," *Opt. Lett.*, vol. 20, pp. 866–868, 1995.

[3] G. Millot, E. Seve, S. Wabnitz, and M. Haelterman, "Observation of induced modulational polarization instabilities and pulse-train generation in the normal-dispersion regime of a birefringent optical fiber," *J. Opt. Soc. Amer. B*, vol. 15, pp. 1266–1277, 1998.

[4] G. P. Agrawal, *Nonlinear Fiber Optics*. San Diego, CA, USA: Academic, 2001.

[5] P. Kockaert, M. Haelterman, S. Pitois, and G. Millot, "Isotropic polarization modulational instability and domain walls in spun fibers," *Appl. Phys. Lett.*, vol. 75, pp. 2873–2875, 1999.

[6] T. Gottschall *et al.*, "Fiber-based source for multiplex-CARS microscopy based on degenerate four-wave mixing," *Opt. Exp.*, vol. 20, pp. 12004–12013, 2012.

[7] E. Silvestre, T. Pinheiro-Ortega, P. Andrés, J. J. Miret, and A. Ortigosa-Blanch, "Analytical evaluation of chromatic dispersion in photonic crystal fibers," *Opt. Lett.*, vol. 30, pp. 453–455, 2005.

[8] R. J. Kruhlak *et al.*, "Polarization modulation instability in photonic crystal fibers," *Opt. Lett.*, vol. 31, pp. 1379–1381, 2006.

[9] G. K. L. Wong *et al.*, "Characterization of chromatic dispersion in photonic crystal fibers using scalar modulation instability," *Opt. Exp.*, vol. 13, pp. 8662–8670, 2005.

[10] I. A. Sukhoivanov, S. O. Iakushev, O. V. Shulika, A. Díez, and M. Andrés, "Femtosecond parabolic pulse shaping in normally dispersive optical fibers," *Opt. Exp.*, vol. 21, pp. 17769–17785, 2013.

[11] A. M. Heidt *et al.*, "Coherent octave spanning near-infrared and visible supercontinuum generation in all-normal dispersion photonic crystal fibers," *Opt. Exp.*, vol. 19, pp. 3775–3787, 2011.

[12] M. Heidt, "Pulse preserving flat-top supercontinuum generation in all-normal dispersion photonic crystal fibers," *J. Opt. Soc. Amer. B*, vol. 27, pp. 550–559, 2010.

[13] Hartung, A. M. Heidt, and H. Bartelt, "Design of all-normal dispersion microstructured optical fibers for pulse-preserving supercontinuum generation," *Opt. Exp.*, vol. 19, pp. 7742–7749, 2011.

[14] M. Heidt *et al.*, "High quality sub-two cycle pulses from compression of supercontinuum generated in all-normal dispersion photonic crystal fiber," *Opt. Exp.*, vol. 19, pp. 13873–13879, 2011.

[15] L. E. Hooper, P. J. Mosley, A. C. Muir, W. J. Wadsworth, and J. C. Knight, "Coherent supercontinuum generation in photonic crystal fiber with all-normal group velocity dispersion," *Opt. Exp.*, vol. 19, pp. 4902–4907, 2011.

[16] M. Klimczak *et al.*, "Coherent supercontinuum generation up to 2.3 μm in all-solid soft-glass photonic crystal fibers with flat all-normal dispersion," *Opt. Exp.*, vol. 22, pp. 18824–18832, 2014.

[17] I. A. Sukhoivanov, S. O. Iakushev, O. V. Shulika, E. Silvestre, and Y. M. V. Andrés, "Design of all-normal dispersion microstructured optical fiber on silica platform for generation of pulse-preserving supercontinuum under excitation at 1550 nm," *J. Lightw. Technol.*, vol. 35, no. 17, pp. 3772–3779, Sep. 2017.

[18] A. M. Heidt, J. S. Feehan, J. H. V. Price, and T. Feurer, "Limits of coherent supercontinuum generation in normal dispersion fibers," *J. Opt. Soc. Amer. B*, vol. 34, pp. 764–775, 2017.

[19] I. Bravo-Gonzalo, R. D. Engelsholm, M. P. Sørensen, and O. Bang, "Polarization noise places severe constraints on coherence of all-normal dispersion femtosecond supercontinuum generation," *Sci. Rep.*, vol. 8, 2018, Art. no. 6579.

[20] Y. Liu *et al.*, "Suppressing short-term polarization noise and related spectral decoherence in all-normal dispersion fiber supercontinuum generation," *J. Lightw. Technol.*, vol. 33, no. 9, pp. 1814–1820, May 2015.

[21] Q. Lin and G. P. Agrawal, "Vector theory of four-wave mixing: polarization effects in fiber-optic parametric amplifiers," *J. Opt. Soc. Amer. B*, vol. 21, pp. 1216–1224, 2004.

[22] P. Hlubina, M. Szpulak, D. Ciprian, T. Martynkien, and W. Urbanczyk, "Measurement of the group dispersion of the fundamental mode of holey fiber by white-light spectral interferometry," *Opt. Exp.*, vol. 15, pp. 11073–11081, 2017.

[23] R. B. Dyott, *Elliptical Fiber Waveguides*. Ed. Boston, MA, USA: Artech House, 1995.